International Immunopharmacology 75 (2019) 105831

Contents lists available at ScienceDirect

International Immunopharmacology

journal homepage: www.elsevier.com/locate/intimp

Inhibition of inflammatory-molecule synthesis in THP-1 cells stimulated with phorbol 12-myristate 13-acetate by brefelamide derivatives

Gaowa Bai[a,1], Takashi Matsuba[b,1], Haruhisa Kikuchi[c,1], Haorile Chagan-Yasutan[a,d], Hirotoshi Motoda[a], Ryo Ozuru[b], Osamu Yamada[e], Yoshiteru Oshima[c,f], Toshio Hattori[a,*]

[a] Department of Health Science and Social Welfare, Kibi International University, 8 Igamachi, Takahashi 716-8508, Japan
[b] Division of Bacteriology, Department of Microbiology and Immunology, Faculty of Medicine, Tottori University, Yonago, Tottori 683-8503, Japan
[c] Laboratory of Natural Product Chemistry, Graduate School of Pharmaceutical Sciences, Tohoku University, Sendai 980-8578, Japan
[d] Mongolian Psychosomatic Medicine Department, International Mongolian Medicine Hospital of Inner Mongolia, Hohhot, China
[e] Research and Development Center, FUSO Pharmaceutical Institute, Ltd, Osaka 536-8523, Japan
[f] Head Office for Open Innovation Strategy, Tohoku University, Sendai 980-8575, Japan

ARTICLE INFO

Keywords:
Osteopontin
THP-1
Brefelamide
Inhibitor
Tuberculosis

ABSTRACT

Plasma osteopontin (OPN) levels are elevated in tuberculosis patients and may involve granuloma formation. New inhibitors using brefelamide, an aromatic amide isolated from *Dictyostelium* cellular slime molds that may inhibit OPN transcription in A549 cells at 1 μM concentration, were synthesized as compounds C, D, and E. Their inhibitory activity against OPN synthesis in phorbol 12-myristate 13-acetate (PMA)-stimulated THP-1 cells was confirmed using enzyme-linked immunosorbent assay (ELISA), a multicolor immune-fluorescent microscope, and western blot. In the ELISA performed using full-length OPN, each compound showed significant inhibition in culture supernatants with half maximal inhibitory concentration (IC_{50}) values of 1.6, 1.8, and 2.2 μM for C, D, and E, respectively. In another ELISA to detect the immune-related form of OPN, IC_{50} values were 0.6, 1.2, and 2.5 μM for compounds C, D, and E, respectively. The decreases in OPN expression and synthesis were confirmed using immunofluorescence and western blot studies using compound-treated cells or cell lysates. Luminex assay of the supernatants of PMA-treated THP-1 cells showed significant reduction in the synthesis of interleukin (IL)-1β, galectin-9, and tumor necrosis factor (TNF)-α. Elucidation of the detailed mechanisms of the biological activities of these compounds would be necessary; however, they may be used in clinical trials for infectious diseases, inflammatory disorders, and cancer.

1. Introduction

Osteopontin (OPN), a calcium-binding glycophosphoprotein originally isolated from bone, mediates bone remodeling and tissue debridement [1]. OPN has been implicated in pathological and physiological processes such as cell proliferation and endothelial cell migration, and is expressed by macrophages [2,3]. OPN also plays an important role in immunity, inflammation, and tumor progression as well as cell viability [4,5], adhesion, proliferation, invasion, and apoptosis in tissue fibrosis [6], by binding to their receptors with integrin and CD44 variants [7]. Previously, we reported the upregulation of OPN in the plasma of adult T cell leukemia and dengue patients, implying its role in disease progression [3,8].

OPN expression was also observed in the granuloma of *Mycobacterium tuberculosis* (MTB) infected individuals [9], and a high level of plasma OPN was confirmed in subjects with MTB from the Philippines [10] and Indonesia [9]. Full-length OPN (FL-OPN), its intact form, serves as a protease(s) cleavage target. During this process, fragments of OPN are produced. Among these fragments, proteolytic cleavage of FL-OPN by thrombin (between Arg168 and Ser169) generates the functional fragment, N-terminal thrombin-cleaved OPN (tr-OPN), which contains cryptic binding sites for the integrins, α9β1 and α4β1, enhancing tr-OPN attachment to integrin. Increases in tr-OPN levels have been reported in the recovery phase of dengue virus (DENV) infection. Furthermore, another OPN form, undefined OPN (Ud-OPN), was detected in DENV infections when a different enzyme-linked immunosorbent assay (ELISA) system was employed [8].

Higher plasma concentrations of Ud-OPN, but not FL-OPN or tr-

* Corresponding author.
E-mail address: hattorit@kiui.ac.jp (T. Hattori).
[1] These authors contributed equally to this work.

https://doi.org/10.1016/j.intimp.2019.105831
Received 2 May 2019; Received in revised form 13 July 2019; Accepted 12 August 2019
Available online 19 August 2019
1567-5769/

OPN, positively correlates with neutrophil numbers and negatively correlates with TB-specific memory T cell numbers [11], and Ud-OPN is dependent on phorbol 12-myristate 13-acetate (PMA)-stimulation, indicating Ud-OPN represent immune-related form of OPN [12].

It is also known that other enzymes such as matrix metalloproteinases (MMPs) can cleave OPN at non-thrombin cleavage sites [13,14]. Accumulation of α4β1 and other integrin-bearing cells is reported in MTB infection [15]. Recently, we showed that small amounts of FL-OPN and tr-OPN were detected in the supernatants of non-PMA-stimulated THP-1 cells using ELISA, with increased levels of all forms, including undefined Ud-OPN, in these cells [12]. Brefelamide has been reported to inhibit OPN expression in A549 cells at a concentration of 50 μM using an OPN promoter reporter assay [16]. We also reported that brefelamide (compound A) and its methyl ether derivative (compound B) suppressed OPN production in DENV-infected THP-1 cells and also inhibited DENV replication [17]. Recently, we developed three novel derivatives (C–E) which exhibited inhibitory activity at lower concentrations and disclosed their different activities.

2. Materials and methods

2.1. Chemicals

Brefelamide (Fig. 1A) is an aromatic amide isolated from methanol extracts of *Dictyostelium brefeldianum* and *D. giganteum* slime mold fruiting bodies [18]; its derivative is referred to as compound B (Fig. 1B), which contains a methyl ether group (–OCH_3) [17]. Compounds C, D, and E were newly synthesized by maintaining the position of the benzene rings, carbonyl groups, and amino groups in brefelamide to enhance its biological activity (Fig. 1C–E). The compounds were dissolved in dimethyl sulfoxide (DMSO) at a concentration of 50 mmol/l and stored at −20 °C. Aliquots of the stock solutions were subsequently diluted to the indicated concentrations before use to treat the cells.

2.2. Cell lines and culture

A549 cells and human THP-1 cells derived from acute monocytic leukemia patients were obtained from the American Type Culture Collection (Manassas, VA, USA). Cells were maintained in Dulbecco's modified Eagle's medium or Roswell Park Memorial Institute (RPMI) 1640 medium (Wako Pure Chemical Industries Ltd., Osaka, Japan), in the presence of 10% fetal bovine serum (Thermo Fisher Scientific, Waltham, MA, USA), 50 U/ml penicillin and streptomycin in a 5% CO_2 humidified atmosphere. PMA (Wako Pure Chemical Industries) (30 ng/ml) was used to induce OPN expression.

2.3. Plasmids transient transfection and luciferase assay

The reporter vector, pOPN1-luc, has been previously described [16]. A549 cells were seeded in 12-well plates at 1×10^5 in 1 ml medium/well, 24 h before transfection. The indicated plasmid DNA was transfected into cells with Effectene Transfection Reagent (Qiagen, Venlo, PL, NLD). For each transient transfection, pRL-TK vector (Promega, Madison, WI, USA) was co-transfected as an internal control to normalize transfection efficiency. Cells were harvested at 48-h post-transfection, and the cell lysates prepared for the luciferase assay with Dual-Luciferase Reporter Assay System (Promega) according to the manufacturer's instructions. Luciferase activity was measured using a GloMax® 20/20 luminometer (Promega). Cell viabilities were tested using cell proliferation reagent (Takara Bio, Shiga, Japan) according to the manufacturer's instructions. The half maximal inhibitory concentration (IC_{50}) of compounds was determined from the dose-response curve as described previously [16].

2.4. Effect of compounds on PMA-stimulated THP-1 cells

THP-1 cells were seeded in 24-well tissue culture plates at a density of 7.2×10^4/well in 1 ml for 24 h at 37°C in a humidified 5% CO_2 atmosphere. The following day, the compounds, which had final concentrations ranging from 1.25 to 5 μM were added simultaneously or 2 h before the addition of PMA (30 ng/ml). After incubation for 48 h, culture supernatants were obtained for ELISA. Then, 25 cm^2 flasks and four-well chamber glass slides (Nunc Lab-Tek™, Thermo Fisher Scientific, MA, USA) were used for western blot and immunofluorescence studies, respectively. An equal volume of medium containing 10 μM of each compound was added to each culture before the addition of PMA. After 2 h, an equal volume of medium containing 60 ng/ml PMA and 5 μM of each compound was added, distributed to each flask (2.5×10^6/flask in 5 ml), and the wells (2×10^5/well in 0.415 ml) at a final density of 5×10^5/ml; incubation was performed for 48 h. The cells were subjected to western blot and immunofluorescence analyses as previously described [15]. The cell viability was tested using the CellTiter 96 Aqueous Non-Radioactive Cell Proliferation System (Promega). Cells were seeded in 96-well tissue culture plates at a density of 2×10^4/well in 50 μl complete medium followed by the addition of compounds and PMA (2 h later) to each well. After incubation for 48 h, 20 μl per well of 3-(4,5-dimethyl-2-yl)-5-(3-carboxymethoxyphenyl)2-(4-sulfophenyl)-2H-tetrazolium salt/phenazine methosulfate solution was added to each well, followed by incubation for 4 h. The absorbance at 492 nm was recorded using an ELISA plate reader (Multiskan FC, Thermo Scientific). The IC_{50} value was determined by identifying the X-axis value corresponding to N-half of the difference between the maximum and minimum absorbance values using GraphPad Prism 7 software (GraphPad Inc., San Diego, CA, USA) as described previously [17].

2.5. ELISA

To identify FL-OPN, an ELISA kit (JP27158, IBL, Gunma, Japan)

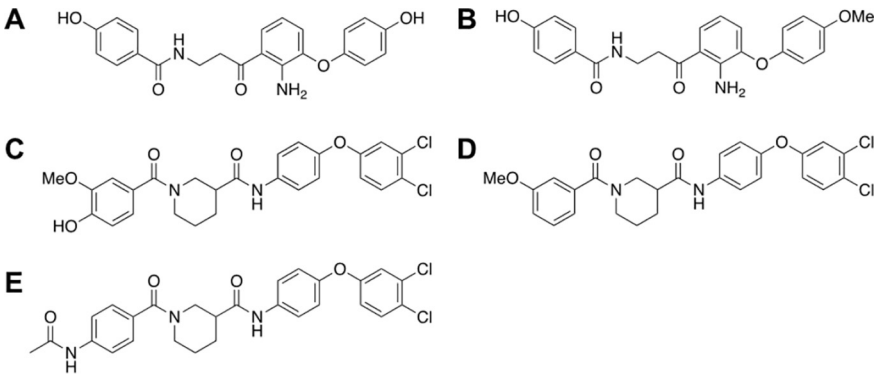

Fig. 1. Chemical structures of the synthesized brefelamide derivatives.

was used [3]. In the FL-OPN kit, O-17, a polyclonal rabbit antibody specific to the N-terminus of OPN was used as the capture antibody, and the mouse monoclonal antibody, 10A16, served as the detector antibody. Ud-OPN in culture supernatants were determined using the Human OPN DuoSet ELISA Development System kit (R&D Systems, Minneapolis, MN, USA) [8]. The proprietary capture monoclonal antibody and the detection polyclonal antibodies in this ELISA kit were both generated against recombinant human OPN (NS0-derived; amino acids, Ile17-Asn300); the epitopes for these antibodies were not disclosed. The amount of the synthesized OPN was calculated based on viable cell numbers, which were determined with the Cell Titer 96 Aqueous Non-Radioactive Cell Proliferation System as described previously [17].

2.6. Immunofluorescence

PMA-stimulated THP-1 cells cultured with compounds on four-well chambered glass slides (Nunc Lab-Tek™, Thermo Fisher Scientific, MA, USA) were fixed with 4% (w/v) paraformaldehyde in phosphate-buffered saline (PBS) -]) for 20 min at 4 °C. Cells were incubated with PBS (−) containing 0.1% (v/v) Triton-X100 for 5 min at room temperature, blocked with PBS (−) containing 5% (v/v) normal goat serum for 1 h, and incubated with each of the appropriate primary antibodies, O-17 (rabbit, 1:400 dilution; IBL, Gunma, Japan) and 34E3 (mouse, 1:400 dilution; IBL). The secondary antibodies, goat anti-rabbit IgG (H + L)-AF488 and F(ab′)2-goat anti-mouse IgG (H + L)-Alexa Fluor ® 546 (AF546), were purchased from Thermo Fisher Scientific (MA, USA). For nuclear staining, 4′,6-diamidino-2-phenylindole (DAPI) was used. The primary and secondary antibodies and DAPI were diluted to 0.25 μg/ml, 5 μg/ml, and 1 μg/ml, respectively with PBS (−) containing 1% (w/v) BSA. Each reagent was incubated for 1 h at room temperature followed by washing twice with PBS (−). Cover slips were mounted onto the glass slides and images captured using a BZ-X700 fluorescence microscope (Keyence, Osaka, Japan). Quantification was performed using the Fiji program [19]. The DAPI signals as numbers of cells and O-17 or 34E3 signals were analyzed. The fluorescent images were divided into each RGB channels, and converted into 16-bit grayscale images. The blue channel (DAPI) signals were selected using the auto-threshold and counted using the menu command of Analyze Particle. The intracellular signals of green (O-17) or red (34E3) channels were selected using the manual threshold and similarly analyzed.

2.7. Western blot analysis

Washed PMA-stimulated THP-1 cells (2.5×10^6) cultured with or without the test compounds were lysed on ice for 15 min in 100 μl of the lysis buffer provided in the WSE-7420 EzRIPA Lysis kit (ATTO Corporation, Tokyo, Japan) as described previously [12]. The supernatants were then processed by centrifugation at 14,000 × *g* for 15 min, according to the manufacturer's protocol. Protein concentration was then determined using the Bradford method (Takara Bio Inc.). Then, 8 μg of protein from each sample was separated using sodium dodecyl sulfate-polyacrylamide gel electrophoresis (SDS-PAGE) using standard 5–20% gradient gels, followed by western blot analysis using a semi-dry transfer apparatus (Bio Craft, Tokyo, Japan). Antibodies were diluted using 1% (v/v) cold fish gelatin (Sigma-Aldrich Co. LLC, St. Louis, MO, USA), 10 mM Tris HCl (pH 8), 150 mM NaCl. The O-17 (1 μg/ml), 34E3 (1 μg/ml), and anti-actin (1:10,000 dilution; A5316, Sigma-Aldrich Co. LLC, St. Louis, MO, USA) antibodies were used as the primary antibodies. Bound primary antibodies were reacted with horseradish peroxidase-conjugated goat anti-rabbit IgG or anti-mouse IgG (1:10,000 dilution; Sigma-Aldrich Co. LLC, St. Louis, MO, USA) antibodies, and were visualized using a TMB membrane peroxidase substrate system (Kirkegaard & Perry Laboratories, Inc., Gaithersburg, MD, USA) according to the manufacturer's protocol.

2.8. Luminex assay

Culture supernatants for the ELISA measurement were subjected to a Luminex assay using CD40L, IL-1α, IL-6, TNF-α, galectin-9, IL-1β, IL-15, GM-CSF, IL-1ra, and TGF-α, which have been reported to be induced in THP-1 cells by PMA [20]. These inflammatory proteins were measured using a human premixed multi-analyte kit (LXSAHM; R&D systems, Minneapolis, MN, USA) using a Bio-Plex™ 200 system (Bio-Rad Laboratories, Inc., Hercules, CA, USA). The cell viability consistently exceeded 90% after culture as determined using the Cell Titer 96 Aqueous Non-Radioactive Cell Proliferation System. The data were analyzed using Bio-Plex Manager™ software version 6.1 (Bio-Rad Laboratories, Inc.). The inhibition (%) was calculated as [1 − (compound value / control value)] × 100, in which the control sample was from the culture treated with DMSO-PMA. The heatmaps of inhibition (%) of each protein cultured with the test compounds were generated using GraphPad Prism version 7 (GraphPad Software Inc. San Diego, CA, USA).

2.9. Statistical analysis

Unpaired *t*-tests (two-tailed) were used to compare the results from the compound- and non-treated PMA-stimulated THP-1 cells. *P*-values < 0.05 were considered statistically significant and all statistical analyses were performed using GraphPad Prism software, version 7.

3. Results

3.1. Inhibition of OPN expression by brefelamide

Luciferase expression level in A549/OPN-luc cells was dose-dependently suppressed by the compounds and compound B showed the highest IC_{50} among the other compounds (Table 1). The activities of compound B have already been reported [17], whereas compounds C, D, and E were newly synthesized as described in the Materials and methods section.

3.2. ELISA

OPN in the supernatant of cells cultured with PMA and three concentrations (5, 2.5, 1.25 μM) of the newly-developed compounds was measured using ELISA. In the ELISA of FL-OPN, compound B did not exert inhibitory activity, C showed dose-dependent inhibitory activity, and D and E suppressed the synthesis of FL-OPN. The IC_{50} values of C, D, and E were 2.6, 2.3, and 3.1 μM, respectively. Next, we compared the effect of the compounds on FL-OPN and Ud-OPN (Fig. 2). Cell were pretreated with the compounds 2 h before PMA addition and the IC_{50} values of compounds C, D, and E were 1.6, 1.8, and 2.2 μM, respectively, for FL-OPN, indicating that pretreatment was more effective. The compounds also showed inhibitory activity in the Ud-OPN assay with IC_{50} values of 0.6, 1.2, and 2.5 μM for compounds C, D, and E respectively. The cell viability after culturing PMA-THP-1 cells with the compounds did not change significantly (Supplementary Fig. 1).

Table 1
Transcription inhibitory activity of test compounds.

Compound	OPN-luc IC_{50} (μM)
B	10.2
C	1
D	1.1
E	1.2

OPN-luc, luciferase expression in A549/OPN-luc cells.
IC_{50}, half maximal inhibitory concentration.

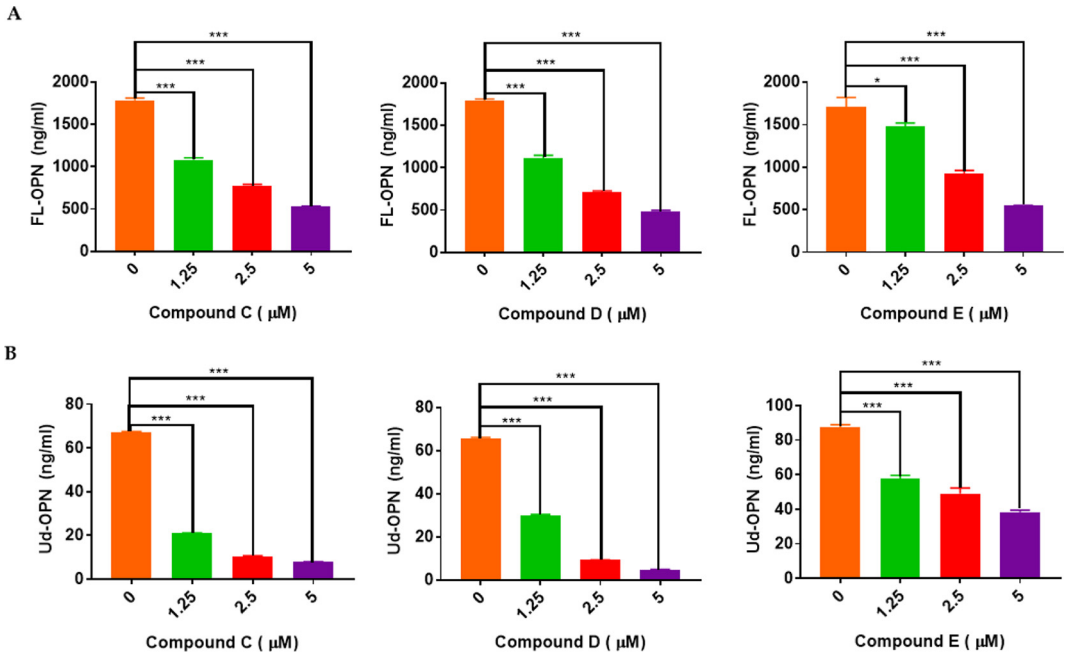

Fig. 2. Effects of compounds C, D, and E on OPN synthesis. (A) FL-OPN and (B) Ud-OPN were studied. ***$P < 0.001$, unpaired *t*-tests (two-tailed), Prism software.

3.3. Immunofluorescence study

Multicolor immunofluorescence analysis of OPN in the compound-treated PMA-stimulated THP-1 cells was performed. The characterization of each antibody in PMA-stimulated THP-1 cells was previously described [12]. Polyclonal rabbit antibody, O-17, specific to the N-terminus of OPN (Ile17-Gln31) and a mouse monoclonal antibody, 34E3, specific to the epitope Ser162-Arg168, which is exposed by thrombin digestion were used [21]. Cells were pretreated with compounds C and D (5 μM), 2 h before PMA addition, and both apparently suppressed cytoplasmic staining of O-17.

Immuno-fluorescence signals of the digital microscopic images were numerically analyzed using Fiji. OPN staining was decreased to almost half by compounds C, D, and E. A few cells were positive for 34E3 staining in control cells, whereas no positively stained compound-treated cells were observed (Fig. 3).

3.4. Western blot analysis

To confirm the effect of these compounds on OPN protein expression, we utilized two antibodies that identify different epitopes of OPN. A definitive band was observed in PMA-treated cells but not in cells cultured in medium alone (Fig. 4). The intensities of actin bands were the same, indicating that comparable amounts of cell extracts were loaded. FL-OPN (70 kDa band) and smaller fragments (50 and 55-kDa bands) were detected by O-17. The apparent reduction of these bands corresponding to full-length OPN was observed in the compound-treated PMA-THP-1 cells. Furthermore, 34E3 showed a 20 kDa band as described previously [12] and no apparent change in expression was observed between control and compound-treated.

3.5. Luminex assay

We previously found that the expression levels of 1382 genes were altered by ≥1.5-fold after exposing A549 cells to brefelamide, and they were distributed into distinct functional groups including those involved in proliferation and cell motility [16]. Therefore, we determined whether compounds also affected the synthesis of other inflammatory molecules using a Luminex assay. Among nine investigated molecules,

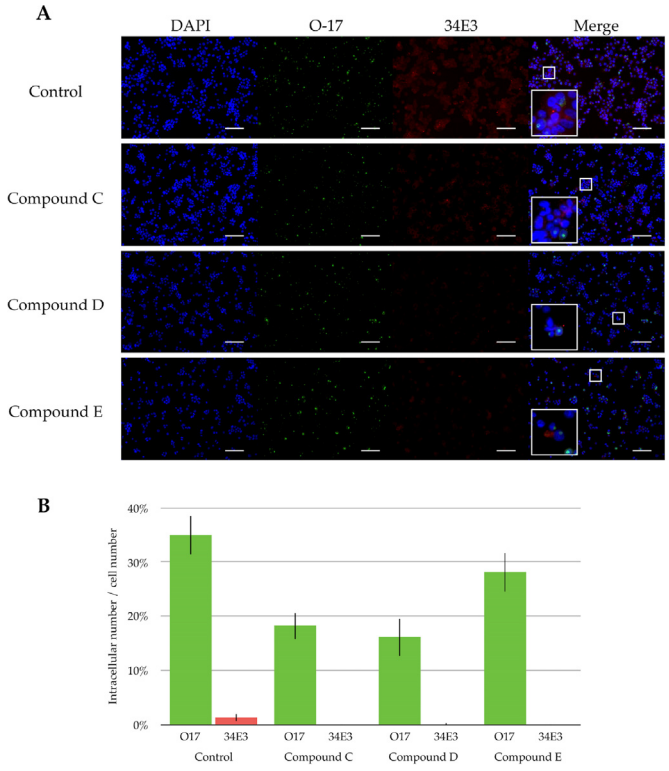

Fig. 3. A. Two-color analysis of compound-treated PMA-stimulated THP-1 cells. O-17 (AF488: green) and 34E3 (AF546: red) were used (×200). Micrograph scale bars represent 100 μm. B. The numerical representation of fluorescence in the particle analysis of Fiji. Fluorescence obtained with O-17 and 34E3 is shown. (For interpretation of the references to color in this figure legend, the reader is referred to the web version of this article.)

compounds significantly suppressed IL-1β production. The synthesis of galectin-9 and TNF-α was also significantly suppressed. In contrast, the expression levels of GM-CSF, IL-6, and TGF-α were not affected (Table 2, Fig. 5).

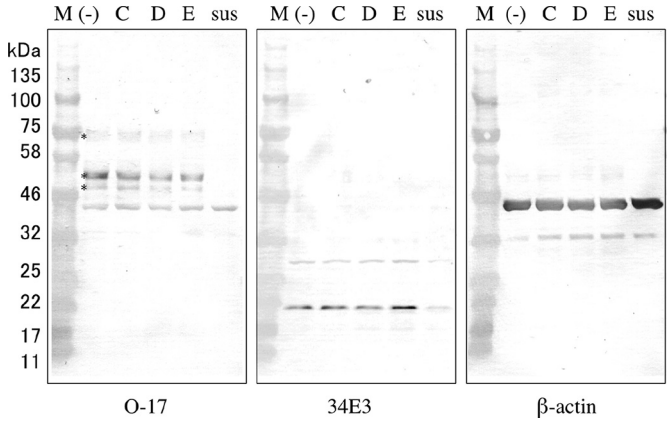

Fig. 4. Western blot analysis of lysates of PMA-stimulated THP-1 cells cultured with the indicated compounds; O-17, 34E3, and anti-β-actin antibodies were used. Cells were cultured with 30 ng/ml PMA for 2 days with the compounds (5 μM C, D, and E), and the cell lysates were subjected to SDS-PAGE (5–20%) followed by immunostaining using an immunodetection kit. M, marker; (−), PMA-THP-1 cells cultured without compound; C, D, and E, PMA-THP-1 cells cultured with compounds C, D or E, respectively; sus, THP-1 cells cultured in PMA-free medium. *Bands corresponding to FL-OPN (70, 55, and 50 kDa).

4. Discussion

In this study, we confirmed that the new compounds generated from brefelamide, which was reported to inhibit OPN expression and protein synthesis at 50 μM, exhibited inhibition at lower concentrations (< 1 μM) in transcription assays (Table 1). Brefelamide is known to induce Smad 4, which is associated with TGF-β signaling, followed by inhibition of OPN synthesis [16]. Compound B had the highest IC_{50} based on the transcription assay. In the ELISA of FL-OPN, C and D showed lower IC_{50} values than E did. Unexpectedly, higher inhibition was observed with Ud-OPN ELISA than with FL-OPN ELISA in compound C- and D-treated cells. The antibody to the N-terminus of OPN revealed that O-17 markedly suppressed OPN synthesis in the compound-treated THP-1 cells in both the immunofluorescence assay and western blot analysis. In the immunofluorescence study, low expression of the 34E3 signal, which is specific to the thrombin-cleaved site SVVYGLR was observed but not after compound treatment. This epitope was deemed a thrombin cleavage site and was also found in PMA-stimulated THP-1 cells as previously reported [12]. Cleaved or modified products or both exhibit greater biological activities by binding to different proteins in the integrin family [21]. In previous studies in patients with pulmonary TB, Ud-OPN showed a negative correlation with the number of ESAT-6-specific IFN-γ spot-forming cells, and a positive correlation with neutrophil numbers, whereas FL-OPN and tr-OPN did not show such correlations [11]. These findings indicate that Ud-OPN may possess more immune-related functions than FL-OPN and tr-OPN; the molecular size of OPN in the Ud-OPN ELISA is unknown. In a previous experiment, Ud-OPN levels were found to decrease following the removal of PMA from the culture, while synthesis of full-length OPN and tr-OPN continued, indicating that the Ud-OPN synthesis was PMA–dependent [12]. Following PMA stimulation, cells express proteases [22], and degradation of OPN may be facilitated but the underlying mechanisms by which these molecules participate in Ud-OPN synthesis are not known.

The Luminex assay clearly showed the effects of these compounds on various molecules and the most pronounced effect was seen on IL-1β production. OPN and IL-1β are reported to be synthesized in *Porphyromonas gingivalis*-infected THP-1 cells and neutralization of OPN by the antibody abrogated IL-1β synthesis, indicating IL-1β synthesis was dependent on OPN [23]. On the other hand, IL-1β is expressed in primary lung fibroblast and promotes OPN synthesis through the activity of the mitogen-activated protein kinase member extracellular

Table 2
Effects of compounds on the synthesis of inflammatory molecules by PMA-THP-1 cells.

	w/o[#]	Compound C						Compound D						Compound E					
		1.25 μM[$]		2.5 μM		5 μM		1.25 μM		2.5 μM		5 μM		1.25 μM		2.5 μM		5 μM	
		Median	*p*	Median	*p*	Median	*p*	Median	*p*	Median	*p*	Median	*p*	Median	*p*	Median	*p*	Median	*p*
CD40L	583[%]	571	ns[&]	493	0.0220	457	0.0070	493	0.0160	487	0.0270	363	0.0008	529	ns	517	0.0423	445	0.0050
Galectin-9	4489	2747	0.0001	2295	< 0.0001	1805	< 0.0001	2333	< 0.0001	2159	< 0.0001	2104	< 0.0001	3034	< 0.0001	2325	< 0.0001	2028	< 0.0001
GM-CSF	2.41	3.60	ns	3.60	ns	2.76	ns	4.11	ns	3.44	ns	2.08	ns	4.45	ns	2.93	ns	2.76	ns
IL-1α	148	130	ns	130	ns	80	0.0067	109	ns	108	0.0332	59	0.0049	120	0.0331	97	0.0455	84	0.0145
IL-1β	977	637	< 0.0001	429	< 0.0001	267	< 0.0001	422	< 0.0001	322	< 0.0001	182	< 0.0001	821	< 0.0001	570	< 0.0001	381	< 0.0001
IL-6	1.85	2.61	ns	1.82	ns	2.48	ns	2.22	ns	2.66	ns	1.66	ns	2.48	ns	2.15	ns	1.82	ns
IL-15	33	33	ns	30	ns	28	ns	31	ns	28	ns	23	0.0021	31	ns	29	ns	28	0.0353
TGF-α	7.62	7.09	ns	7.41	ns	7.52	ns	7.41	ns	6.45	ns	7.09	ns	7.52	ns	7.31	ns	7.20	ns
TNF-α	119	105	0.0164	83	0.0005	67	0.0001	84	0.0005	75	0.0002	56	< 0.0001	120	ns	98	0.0106	73	0.0002

[#] Unpaired *t*-test (two-tailed) were used to assess compound-treated and untreated cells (w/o nd).
[$] Three different concentrations of each compound (1.25, 2.5, and 5 μM) are shown.
[%] Results are median levels (pg/ml) of triplicate samples and *P*-values.
[&] Not significant.

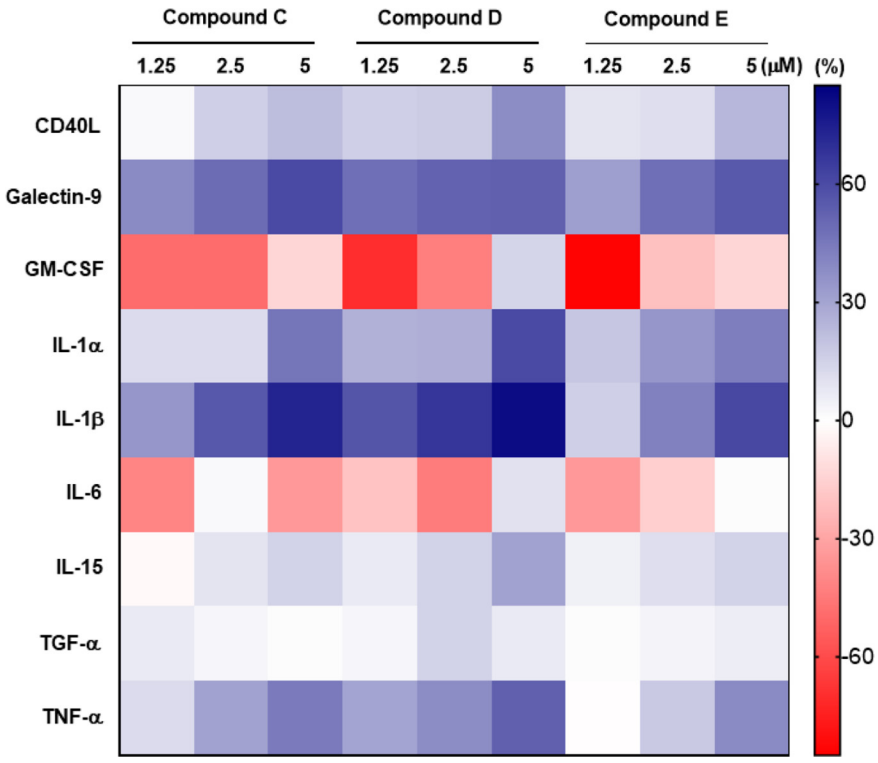

Fig. 5. Heatmap of inhibition (%) measured using Luminex assay. Effects of compounds C, D, and E on indicated biomarkers are shown. All compounds considerably inhibited galectin-9 and IL-1β. The percentage inhibition is displayed as colors ranging from red to blue as shown in legend key. (For interpretation of the references to color in this figure legend, the reader is referred to the web version of this article.)

signal-regulated kinase 1 and 2 (ERK1/2) [24]. Furthermore, brefelamide inhibited epidermal growth factor (EGF)-induced phosphorylation of ERK in human astrocytoma cells [25]. In human lung cells (A549), brefelamide was found to increase Smad4 and restoration of Smad4/TGF may inhibit OPN synthesis [16]. Therefore, further bi-chemical analysis of compound-treated THP-1 cells would be necessary.

The suppression of Ud-OPN synthesis, which was presumed to include the cleaved form, was more prominent than that of the full-length form, indicating that the compound may affect the cleaved pathway. It is noteworthy that both IL-1β [26] and the cleaved form of OPN [27] were generated by caspase 8 and it would be expedient to study the effect of these compounds on caspase and MMP-9. Because IL-1β is a critical mediator of the inflammatory response, OPN was proposed to be a potential drug target to rescue inflammation [23]. The mechanism by which galectin-9 synthesis is involved in OPN synthesis is not clear but the levels of OPN and galectin-9 were significantly correlated with MTB infections [11]. It is also known that Tim3–galectin-9 interaction activates mouse macrophages and stimulates bactericidal activity by inducing caspase-1-dependent IL-1β secretion [28]. Therefore, the marked suppression of IL-1β might be caused by the decrease in both OPN and galectin-9. Furthermore, it was revealed that IL-1β plays a major role in host resistance to MTB by a mechanism independent of TLR signaling or caspase-1 in mice [29].

The synthesis of TNF-α was also significantly suppressed by these compounds, and both IL-1β and TNF-α are proposed to contribute to granuloma formation, macrophage activation, and host protection during MTB infection [30].

It should also be noted that the immune check-point molecule, programmed death ligand 1 (PD-L1), is dependent on OPN in THP-1 cells, which may restore T cell activation [31]. More detailed analysis of OPN metabolism in PMA-stimulated THP-1 cells is required to clarify the biological roles of these compounds, because strict culture conditions of THP-1 after treatment of PMA would be a more reliable model of macrophages as reported previously [32].

In addition to our group, other researchers have reported elevated OPN levels and its association with the severity of MTB infection [9–11,33]. OPN was also reported to serve as a reliable prognostic indicator of improvement during the early treatment of pulmonary TB [34]. Furthermore, it was suggested that the level of OPN protein expression correlates with effective immune and inflammatory responses [35].

Immuno-histochemical analysis has demonstrated the presence of OPN in granuloma and its association with macrophages; the Ud-OPN levels were positively and negatively associated with neutrophil and lymphocyte numbers, respectively [11]. Increased OPN expression was also found to be associated with silicosis, another granulomatous disease. Therefore, OPN is believed to participate in granuloma formation [36].

We have clearly demonstrated that the new compounds effectively inhibited OPN synthesis *in vitro* at low concentration. Therefore, investigating the effects of these compounds on MTB infection *in vivo* would be an interesting future project. TB therapy is hampered by many factors and granuloma formation may be one of the major causes of poor drug delivery, leading to drug resistance. The development of adjunctive, granuloma-targeted therapies similar to other host-directed therapies may be beneficial in increasing the availability of approved drugs to aid treatment and prevention of TB. Neutrophil numbers, which are associated with OPN levels, are known risk factors of TB [37,38].

Statins, which suppress OPN production [39] have been associated with a reduced risk of developing active TB in some studies [40]. Therefore, the newly generated compounds described here would be potentially useful in host-directed therapy.

5. Conclusions

In conclusion, we have demonstrated that the novel brefelamide-derived compounds investigated in this study suppressed OPN, IL-1β, galectin-9, and TNF-α production in PMA-stimulated THP-1 cells. The usefulness of compounds should be further assessed in clinical trials for infectious diseases, inflammatory disorders, and cancers.

Supplementary data to this article can be found online at https://doi.org/10.1016/j.intimp.2019.105831.

Author contributions

Methodology, Y.O. and H.K.; investigation, O.Y., G.B., R.O. and T.M.; formal analysis, O.Y., G.B., R.O. and T.M; data curation, T.M., H.C.-Y., O.Y. H.M. and T.H.; writing, T.M., O.Y. H.C.-Y. and T.H.

Funding

This research was funded by the Research Program on Emerging and Re-emerging Infectious Diseases from the Japan Agency for Medical Research and Development (AMED JP18fk0108042h0002), and partially supported by the Japan Society for the Promotion of Science (JSPS) Grants-in-Aid for Scientific Research (KAKENHI), Grant Number JP17H01690.

Declaration of competing interest

The authors declare no conflict of interest.

References

[1] C.M. Giachelli, S. Steitz, Osteopontin: a versatile regulator of inflammation and biomineralization, Matrix Biol. 19 (2000) 615–622, https://doi.org/10.1016/S0945-053X(00)00108-6.

[2] D.R. Senger, S.R. Ledbetter, K.P. Claffey, A. Papadopoulos-Sergiou, C.A. Peruzzi, M. Detmar, Stimulation of endothelial cell migration by vascular permeability factor/vascular endothelial growth factor through cooperative mechanisms involving the alphavbeta3 integrin, osteopontin, and thrombin, Am. J. Pathol. 149 (1996) 293–305.

[3] H. Chagan-Yasutan, K. Tsukasaki, Y. Takahashi, S. Oguma, H. Harigae, N. Ishii, J. Zhang, M. Fukumoto, T. Hattori, Involvement of osteopontin and its signaling molecule CD44 in clinicopathological features of adult T cell leukemia, Leuk. Res. 35 (2011) 1484–1490, https://doi.org/10.1016/j.leukres.2011.05.011.

[4] M. Mazzali, T. Kipari, V. Ophascharoensuk, J.A. Wesson, R. Johnson, J. Hughes, Osteopontin—a molecule for all seasons, QJM 95 (2002) 3–13, https://doi.org/10.1093/qjmed/95.1.3.

[5] M.K. El-Tanani, F.C. Campbell, V. Kurisetty, D. Jin, M. McCann, P.S. Rudland, The regulation and role of osteopontin in malignant transformation and cancer, Cytokine Growth Factor Rev. 17 (2006) 463–474, https://doi.org/10.1016/j.cytogfr.2006.09.010.

[6] A. Kato, T. Okura, C. Hamada, S. Miyoshi, H. Katayama, J. Higaki, R. Ito, Cell stress induces upregulation of osteopontin via the ERK pathway in type II alveolar epithelial cells, PLoS One 9 (2014) e100106, , https://doi.org/10.1371/journal.pone.0100106.

[7] J.E. Murphy-Ullrich, E.H. Sage, Revisiting the matricellular concept, Matrix Biol. 37 (2014) 1–14, https://doi.org/10.1016/j.matbio.2015.07.005.

[8] H. Chagan-Yasutan, T.L. Lacuesta, L.C. Ndhlovu, S. Oguma, P.S. Leano, E.F. Telan, T. Kubo, K. Morita, T. Uede, E.M. Dimaano, T. Hattori, Elevated levels of full-length and thrombin-cleaved osteopontin during acute dengue virus infection are associated with coagulation abnormalities, Thromb. Res. 134 (2014) 449–454, https://doi.org/10.1016/j.thromres.2014.05.003.

[9] F.M. Hasibuan, B. Shiratori, M.A. Senoputra, H. Chagan-Yasutan, R.C. Koesoemadinata, L. Apriani, Y. Takahashi, T. Niki, B. Alisjahbana, T. Hattori, Evaluation of matricellular proteins in systemic and local immune response to Mycobacterium tuberculosis infection, Microbiol. Immunol. 59 (2015) 623–632, https://doi.org/10.1111/1348-0421.12320.

[10] B. Shiratori, S. Leano, C. Nakajima, H. Chagan-Yasutan, T. Niki, Y. Ashino, Y. Suzuki, E. Telan, T. Hattori, Elevated OPN, IP-10, and neutrophilia in loop-mediated isothermal amplification confirmed tuberculosis patients, Mediat. Inflamm. 2014 (2014) 513263, https://doi.org/10.1155/2014/513263.

[11] B. Shiratori, J. Zhao, M. Okumura, H. Chagan-Yasutan, H. Yanai, K. Mizuno, T. Yoshiyama, T. Idei, Y. Ashino, C. Nakajima, Y. Suzuki, T. Hattori, Immunological roles of elevated plasma levels of matricellular proteins in Japanese patients with pulmonary tuberculosis, Int. J. Mol. Sci. 18 (2016), https://doi.org/10.3390/ijms18010019.

[12] G. Bai, H. Motoda, R. Ozuru, H. Chagan-Yasutan, T. Hattori, T. Matsuba, Synthesis of a cleaved form of osteopontin by THP-1 cells and its alteration by phorbol 12-myristate 13-acetate and BCG infection, Int. J. Mol. Sci. 19 (2018), https://doi.org/10.3390/ijms19020418.

[13] B. Christensen, L. Schack, E. Klaning, E.S. Sorensen, Osteopontin is cleaved at multiple sites close to its integrin-binding motifs in milk and is a novel substrate for plasmin and cathepsin D, J. Biol. Chem. 285 (2010) 7929–7937, https://doi.org/10.1074/jbc.M109.075010.

[14] R. Agnihotri, H.C. Crawford, H. Haro, L.M. Matrisian, M.C. Havrda, L. Liaw, Osteopontin, a novel substrate for matrix metalloproteinase-3 (stromelysin-1) and matrix metalloproteinase-7 (matrilysin), J. Biol. Chem. 276 (2001) 28261–28267, https://doi.org/10.1074/jbc.M103608200.

[15] J.T. Mattila, W. Beaino, P. Maiello, M.T. Coleman, A.G. White, C.A. Scanga, J.L. Flynn, C.J. Anderson, Positron emission tomography imaging of macaques with tuberculosis identifies temporal changes in granuloma glucose metabolism and integrin alpha4beta1-expressing immune cells, J. Immunol. 199 (2017) 806–815, https://doi.org/10.4049/jimmunol.1700231.

[16] J. Zhang, O. Yamada, S. Kida, Y. Matsushita, S. Murase, T. Hattori, Y. Kubohara, H. Kikuchi, Y. Oshima, Identification of brefelamide as a novel inhibitor of osteopontin that suppresses invasion of A549 lung cancer cells, Oncol. Rep. 36 (2016) 2357–2364, https://doi.org/10.3892/or.2016.5006.

[17] D.N. Pascapurnama, H.K. Labayo, I. Dapat, D.D. Nagarajegowda, J. Zhao, J. Zhang, O. Yamada, H. Kikuchi, S. Egawa, Y. Oshima, H. Chagan-Yasutan, T. Hattori, Induction of osteopontin by Dengue virus-3 infection in THP-1 cells: inhibition of the synthesis by brefelamide and its derivative, Front. Microbiol. 8 (2017) 521, https://doi.org/10.3389/fmicb.2017.00521.

[18] H. Kikuchi, Y. Saito, J. Sekiya, Y. Okano, M. Saito, N. Nakahata, Y. Kubohara, Y. Oshima, Isolation and synthesis of a new aromatic compound, brefelamide, from dictyostelium cellular slime molds and its inhibitory effect on the proliferation of astrocytoma cells, J. Org. Chem. 70 (2005) 8854–8858, https://doi.org/10.1021/jo051352x.

[19] J. Schindelin, I. Arganda-Carreras, E. Frise, V. Kaynig, M. Longair, T. Pietzsch, S. Preibisch, C. Rueden, S. Saalfeld, B. Schmid, J.Y. Tinevez, D.J. White, V. Hartenstein, K. Eliceiri, P. Tomancak, A. Cardona, Fiji: an open-source platform for biological-image analysis, Nat. Methods 9 (2012) 676–682, https://doi.org/10.1038/nmeth.2019.

[20] S. Tedesco, F. De Majo, J. Kim, A. Trenti, L. Trevisi, G.P. Fadini, C. Bolego, P.W. Zandstra, A. Cignarella, L. Vitiello, Convenience versus biological significance: are PMA-differentiated THP-1 cells a reliable substitute for blood-derived macrophages when studying in vitro polarization? Front. Pharmacol. 9 (2018) 71, https://doi.org/10.3389/fphar.2018.00071.

[21] S. Kon, Y. Yokosaki, M. Maeda, T. Segawa, Y. Horikoshi, H. Tsukagoshi, M.M. Rashid, J. Morimoto, M. Inobe, N. Shijubo, A.F. Chambers, T. Uede, Mapping of functional epitopes of osteopontin by monoclonal antibodies raised against defined internal sequences, J. Cell. Biochem. 84 (2002) 420–422.

[22] J.H. Kang, J.K. Kim, W.H. Park, K.K. Park, T.S. Lee, J. Magae, H. Nakajima, C.H. Kim, Y.C. Chang, Ascochlorin suppresses oxLDL-induced MMP-9 expression by inhibiting the MEK/ERK signaling pathway in human THP-1 macrophages, J. Cell. Biochem. 102 (2007) 506–514, https://doi.org/10.1002/jcb.21312.

[23] C. Che, J. Liu, J. Yang, L. Ma, N. Bai, Q. Zhang, Osteopontin is essential for IL-1beta production and apoptosis in peri-implantitis, Clin. Implant. Dent. Relat. Res. 20 (2018) 384–392, https://doi.org/10.1111/cid.12592.

[24] D.M. Serlin, P.P. Kuang, M. Subramanian, A. O'Regan, X. Li, J.S. Berman, R.H. Goldstein, Interleukin-1beta induces osteopontin expression in pulmonary fibroblasts, J. Cell. Biochem. 97 (2006) 519–529, https://doi.org/10.1002/jcb.20661.

[25] S. Honma, M. Saito, H. Kikuchi, Y. Saito, Y. Oshima, N. Nakahata, M. Yoshida, A reduction of epidermal growth factor receptor is involved in brefelamide-induced inhibition of phosphorylation of ERK in human astrocytoma cells, Eur. J. Pharmacol. 616 (2009) 38–42, https://doi.org/10.1016/j.ejphar.2009.06.30.

[26] T.P. Monie, C.E. Bryant, Caspase-8 functions as a key mediator of inflammation and pro-IL-1beta processing via both canonical and non-canonical pathways, Immunol. Rev. 265 (2015) 181–193, https://doi.org/10.1111/jmr.12284.

[27] H.J. Kim, H.J. Lee, J.I. Jun, Y. Oh, S.G. Choi, H. Kim, C.W. Chung, I.K. Kim, I.S. Park, H.J. Chae, H.R. Kim, Y.K. Jung, Intracellular cleavage of osteopontin by caspase-8 modulates hypoxia/reoxygenation cell death through p53, Proc. Natl. Acad. Sci. U. S. A. 106 (2009) 15326–15331, https://doi.org/10.1073/pnas.0903704106.

[28] P. Jayaraman, I. Sada-Ovalle, S. Beladi, A.C. Anderson, V. Dardalhon, C. Hotta, V.K. Kuchroo, S.M. Behar, Tim3 binding to galectin-9 stimulates antimicrobial immunity, J. Exp. Med. 207 (2010) 2343–2354, https://doi.org/10.1084/jem.20100687.

[29] K.D. Mayer-Barber, D.L. Barber, K. Shenderov, S.D. White, M.S. Wilson, A. Cheever, D. Kugler, S. Hieny, P. Caspar, G. Nunez, D. Schlueter, R.A. Flavell, F.S. Sutterwala, A. Sher, Caspase-1 independent IL-1beta production is critical for host resistance to Mycobacterium tuberculosis and does not require TLR signaling in vivo, J. Immunol. 184 (2010) 3326–3330, https://doi.org/10.4049/jiuumunol.0904189.

[30] A. O'Garra, P.S. Redford, F.W. McNab, C.I. Bloom, R.J. Wilkinson, M.P. Berry, The immune response in tuberculosis, Annu. Rev. Immunol. 31 (2013) 475–527, https://doi.org/10.1146/annurev-immunol-032712-095939.

[31] Y. Zhang, W. Du, Z. Chen, C. Xiang, Upregulation of PD-L1 by SPP1 mediates macrophage polarization and facilitates immune escape in lung adenocarcinoma, Exp. Cell Res. 359 (2017) 449–457, https://doi.org/10.1016/j.excr.2017.08.028.

[32] W. Chanput, J.J. Mes, H.J. Wichers, THP-1 cell line: an in vitro cell model for immune modulation approach, Int. Immunopharmacol. 23 (2014) 37–45, https://doi.org/10.1016/j.intimp.2-14.08.002.

[33] Y. Koguchi, K. Kawakami, K. Uezu, K. Fukushima, S. Kon, M. Maeda, A. Nakamoto, I. Owan, M. Kuba, N. Kudeken, M. Azuma, S. Yara, T. Shinzato, F. Higa, M. Tateyama, J. Kadota, H. Mukae, S. Kohno, T. Uede, A. Saito, High plasma osteopontin level and its relationship with interleukin-12-mediated type 1 T helper cell response in tuberculosis, Am. J. Respir. Crit. Care Med. 167 (2003) 1355–1359, https://doi.org/10.1164/rccm.200209-1113OC.

[34] Y. Zhu, H. Jia, J. Chen, G. Cui, H. Gao, Y. Wei, C. Lu, L. Wang, T. Uede, H. Diao, Decreased osteopontin expression as a reliable prognostic Indicator of improvement in pulmonary tuberculosis: impact of the level of interferon-gamma-inducible protein 10, Cell. Physiol. Biochem. 37 (5) (2015) 1983–1996 (0.1159/000438559).

[35] G.J. Nau, G.L. Chupp, J.F. Emile, E. Jouanguy, J.S. Berman, J.L. Casanova, R.A. Young, Osteopontin expression correlates with clinical outcome in patients with mycobacterial infection, Am. J. Pathol. 157 (2000) 37–42.

[36] G.J. Nau, P. Guilfoile, G.L. Chupp, J.S. Berman, S.J. Kim, H. Kornfeld, R.A. Young, A

chemoattractant cytokine associated with granulomas in tuberculosis and silicosis, Proc. Natl. Acad. Sci. U. S. A. 94 (1997) 6414–6419, https://doi.org/10.1016/S0002-9440(10)64514-2.

[37] D. Kiran, B.K. Podell, M. Chambers, R.J. Basaraba, Host-directed therapy targeting the Mycobacterium tuberculosis granuloma: a review, Semin. Immunopathol. 38 (2016) 167–183, https://doi.org/10.1007/s00281-015-0537-x.

[38] C. Stek, B. Allwood, N.F. Walker, R.J. Wilkinson, L. Lynen, G. Meintjes, The immune mechanisms of lung parenchymal damage in tuberculosis and the role of host-directed therapy, Front. Microbiol. 9 (2018) 2603, https://doi.org/10.3389/fmicb.2018.02603.

[39] M. Matsuura, T. Suzuki, M. Suzuki, R. Tanaka, E. Ito, T. Saito, Statin-mediated reduction of osteopontin expression induces apoptosis and cell growth arrest in ovarian clear cell carcinoma, Oncol. Rep. 25 (2011) 41–74, https://doi.org/10.3892/or_00001039.

[40] C.C. Lai, M.T. Lee, S.H. Lee, W.T. Hsu, S.S. Chang, S.C. Chen, C.C. Lee, Statin treatment is associated with a decreased risk of active tuberculosis: an analysis of a nationally representative cohort, Thorax 71 (2016) 646–651, https://doi.org/10.1136/thoraxjnl-2015-207052.